

Use of novel echocardiographic techniques to assess right ventricular geometry and function

Elena Surkova^{1,2}, Diletta Peluso¹, Jarosław D. Kasprzak³, Luigi P. Badano¹

¹Department of Cardiac, Thoracic, and Vascular Sciences, University of Padua School of Medicine, Padua, Italy

²Department of Internal Medicine, Samara State Medical University, Samara, Russian Federation

³Department of Cardiology, Medical University of Lodz, Lodz, Poland



Elena Surkova, MD, PhD is a Clinical research fellow at the Department of Cardiac, Thoracic, and Vascular Sciences of the University of Padua School of Medicine in Padua, Italy. Doctor Surkova graduated from Samara State Medical University (Samara, Russia) and completed her PhD there. Main area of Doctor Surkova's research includes utilising advanced imaging techniques in the assessment of cardiac anatomy and functions. She is specifically interested in the deformation imaging and three-dimensional echocardiographic assessment of the right heart. She is a member of Russian Society of Cardiology and the European Society of Cardiology (ESC), a Silver member and Ambassador for the Russian Federation of Heart Imagers of Tomorrow (HIT), and a member of the European Association of Cardiovascular Imaging (EACVI). She has recently been awarded long-term training and research fellowships from the ESC and EACVI. Doctor Surkova has co-authored over 15 papers in peer-reviewed journals.



Diletta Peluso, MD is a PhD fellow at the Department of Cardiac, Thoracic, and Vascular Sciences of the University of Padua, Italy. She obtained her medical degree at the University of Padua in 2007 and then became a specialist in cardiology in 2012. Her main research areas are pulmonary hypertension, three-dimensional echocardiography, and speckle-tracking echocardiography.



Jarosław D. Kasprzak, MD, PhD, FESC, FACC graduated from the Medical University of Lodz and is board certified in internal medicine and cardiology. He is currently the Head of Chair and Department of Cardiology of the Medical University in Lodz, at Bieganski Specialty Hospital. He has held various positions including board member and treasurer responsibilities in the Polish Cardiac Society as well as the Working Group on Echocardiography ESC and European Association of Cardiovascular Imaging. He has chaired the young investigators unit "Club 30" and the Working Group of Echocardiography of the Polish Cardiac Society. Professor Kasprzak has been long involved in pioneering work on novel echocardiographic modalities including three-dimensional echocardiography, contrast echocardiography, and advanced quantitative techniques including speckle tracking and has created an internationally recognised imaging research group at his home university. His current interests include pulmonary hypertension and interventions in structural heart disease. He is an author and reviewer of leading international cardiovascular journals and contributor to global manuals and guidelines.

Address for correspondence:

Dr Elena Surkova, MD, PhD, Department of Cardiac, Thoracic, and Vascular Sciences, University of Padua, Via Giustiniani 2, 35123 Padua, Italy, tel: +39 344 1075905, e-mail: elena.surkova.md@gmail.com

Prof. Jarosław D. Kasprzak, Department of Cardiology, Medical University of Lodz, ul. Kniaziewiczza 1/5, 91–347 Łódź, Poland, fax: +48 42 6539909, e-mail: kasprzak@ptkardio.pl

Received: 02.03.2016 Accepted: 02.03.2016 Available as AoP: 01.04.2016

Kardiologia Polska Copyright © Polskie Towarzystwo Kardiologiczne 2016



Luigi P. Badano, MD, PhD, FESC, FACC currently serves as the director of the echocardiography laboratory and as a professor of cardiovascular imaging at the University of Padua School of Medicine, Padua, Italy. Professor Badano's clinical interests include native and prosthetic valvular heart disease, and right ventricular and atrial function, with research interests in three-dimensional and deformation imaging echocardiography and cardiac mechanics. Professor Badano is a member of the Italian Society of Cardiology, the Italian Society of Cardiovascular Ultrasound, the European Society of Cardiology (ESC), the European Association of Cardiovascular Imaging (EACVI), the American College of Cardiology (ACC), and the American Society of Echocardiography (ASE), and a fellow of the ESC and the ACC. Professor Badano is a regular lecturer at ESC, ACC, ASE, and EuroEcho scientific meetings. He has more than 200 peer-reviewed publications, he has authored seven books about echocardiography and cardiovascular imaging, and was President of the EACVI. He is an honorary member of the British Society of Echocardiography, and the Hungarian and Korean Societies of Cardiology. In 2013, he was awarded the silver medal of the ESC for his clinical and research activity and his commitment as President of the EACVI.

INTRODUCTION

Recent recognition of the right ventricle (RV) as a key player in cardiac physiology and pathophysiology underpins the critical importance of an accurate assessment of its size, geometry, and function. Over the last two decades RV performance has been demonstrated to be an important independent predictor of morbidity and mortality in patients with congenital heart disease, heart failure, pulmonary hypertension, dilated cardiomyopathy, coronary artery disease, left ventricular (LV) dysfunction, respiratory distress syndrome, sepsis, heart transplant, implanted LV assist devices, and even in the population free of cardiovascular diseases [1, 2].

The precise evaluation of the RV by echocardiography is challenging due to its unfavourable location within the thoracic cavity, complex three-dimensional (3D) anatomy, and limited number of well-defined anatomical landmarks. At present, echocardiography remains a cornerstone in RV assessment, being a widely available, safe, fast, and relatively inexpensive modality suitable for various clinical settings including acute conditions and intraoperative monitoring. However, two-dimensional echocardiography (2DE) has a number of important limitations, and under specific conditions it correlates poorly with measurements obtained with cardiac magnetic resonance (CMR), which is considered the standard reference imaging modality for the evaluation of the RV. The introduction of new echocardiographic techniques including two-dimensional speckle-tracking echocardiography (2DSTE) and three-dimensional echocardiography (3DE) helped to achieve a level of accuracy in the assessment of the RV comparable to that obtained by CMR [3].

The following review summarises currently available echocardiographic parameters proposed to assess the RV size, function, and mechanics, their advantages, limitations, and pitfalls in the various clinical settings, with an emphasis on the relative merits of newer echocardiographic techniques and a practical approach to echo data acquisition and analysis.

RIGHT VENTRICULAR ANATOMY AND (PATHO-)PHYSIOLOGY

The following specific morphological and physiological features of the RV should be considered for a better understanding of the existing challenges and pitfalls in RV imaging:

- The RV has a characteristic 3D anatomical structure, being 'wrapped' around the LV with a triangular shape in the frontal plane and a crescent shape in the transversal plane (Fig. 1). Anatomically, the RV is separated into: (i) the inflow tract comprising the tricuspid valve, chordae tendineae, and papillary muscles; (ii) the outflow tract with smooth walls; and (iii) the muscular trabeculated apex. This usually precludes imaging all the parts of the RV in a single 2DE view [4].
- The RV is located just behind the sternum, anterior to the LV apex (Fig. 2). Such a position hampers adequate assessment of the RV including acquisition of complete 3D datasets and affects the image quality [5].
- The RV is significantly more trabeculated than the LV which hinders accurate endocardial delineation and thus accuracy and reproducibility of RV quantitative analysis algorithms [6].
- The RV has a thin free wall (RV mass is around one sixth the mass of the LV) [7] meaning that high spatial resolution is essential for tissue characterisation in non-hypertrophic RV myocardium.
- Three mechanisms contribute to RV pump function: (i) shortening of the longitudinal axis with traction of the tricuspid valve towards the apex; (ii) inward movement of the RV free wall; and (iii) bulging of the interventricular septum (IVS) into the RV during the LV contraction and stretching the free wall of the RV over the septum [4]. For a comprehensive evaluation of RV systolic function and mechanics, an imaging modality should be capable of assessing the relative contribution of these three components.
- Despite significant embryological, morphological, and physiological differences, a close relationship exists between RV and LV function [7, 8]. Noting that around

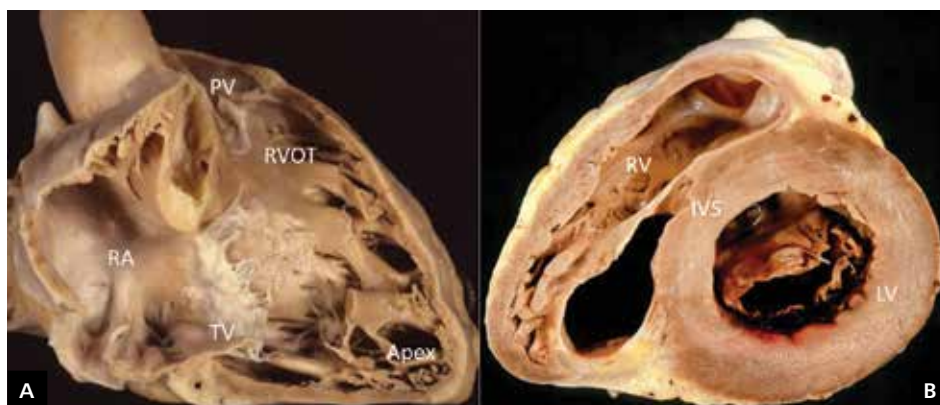


Figure 1. Anatomical specimens of the right ventricle (RV); **A.** Section through the right atrium (RA), RV, and tricuspid valve (TV). Note the triangular shape of the RV in the frontal plane and its three parts: (i) the inflow tract comprising the leaflets of TV, widely separated papillary muscles, and chordae tendineae having accessory attachments to the interventricular septum (IVS) and moderator band; (ii) the muscular trabeculated apex; (iii) and the outflow tract with smooth walls and leaflets of pulmonary valve (PV); **B.** Transversal section of the ventricles. Note the crescent shape of the RV, thin RV free wall, and trabeculated cavity. (Courtesy of Dr. Cristina Basso); LV — left ventricle; RVOT — right ventricular outflow tract

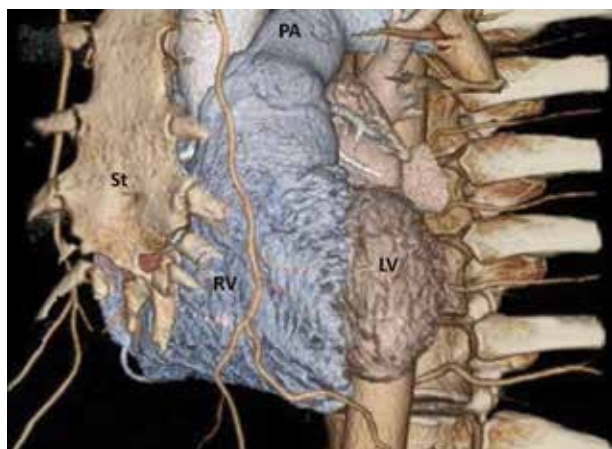


Figure 2. Computed tomography three-dimensional reconstruction of the heart within the chest as "electronic cast" obtained by making soft tissues completely transparent and increasing the opacity of intracavitary contrast. This modality shows the spatial relationships between right ventricle (RV) and other anatomical structures within the thoracic cavity. (Courtesy of Dr. Francesco Faletta); LV — left ventricle; PA — pulmonary artery; St — sternum

one-third of the pressure generated in the RV is determined by LV contraction, any imaging modality should provide accurate information about LV functional status, IVS motion, and interventricular dyssynchrony.

STANDARD ECHOCARDIOGRAPHIC VIEWS OF THE RIGHT VENTRICLE

Six standardised 2DE views should be obtained for a comprehensive assessment of the different segments of the RV

(Fig. 3) [9]. Additional non-standard views may be required for accurate evaluation of specific regions of interest depending on the clinical situation and diagnostic task. In case of discrepancies among the parameters of RV structure and function obtained from the different views, the interpreting physician should consider and integrate all the information contained within the echocardiographic study in order to perform a global assessment of the RV. 3DE is free from 2DE limitations and allows assessment of all three structural components of the RV (inflow, outflow, and apex) in a single dataset, providing information on the RV geometry, volumes, and function without using geometrical assumptions about RV cavity shape.

QUALITATIVE ASSESSMENT

A qualitative evaluation of the RV includes the assessment of its shape, position, and motion of the IVS, visual estimation of the RV size (in comparison with LV), and assessment of wall motion abnormalities. The crescent shape of the RV in the normal heart alters in overload conditions due to flattening of the IVS (Fig. 4). The LV takes the shape of the letter 'D', which may be a sign of RV volume overload if the flattening of the septum is present only during diastole, or RV pressure overload if the septum flattening persists during systole. At the advanced stage of the disease, an altered shape of the RV may be maintained during the entire cardiac cycle. The eccentricity index (EI) had been suggested for quantitative assessment of changes in LV shape (Fig. 4). Normal individuals have a value of one, both during systole and diastole indicative of the circular shape of the LV in transverse sections. An EI higher than one at end diastole is highly suggestive for RV volume overload, and

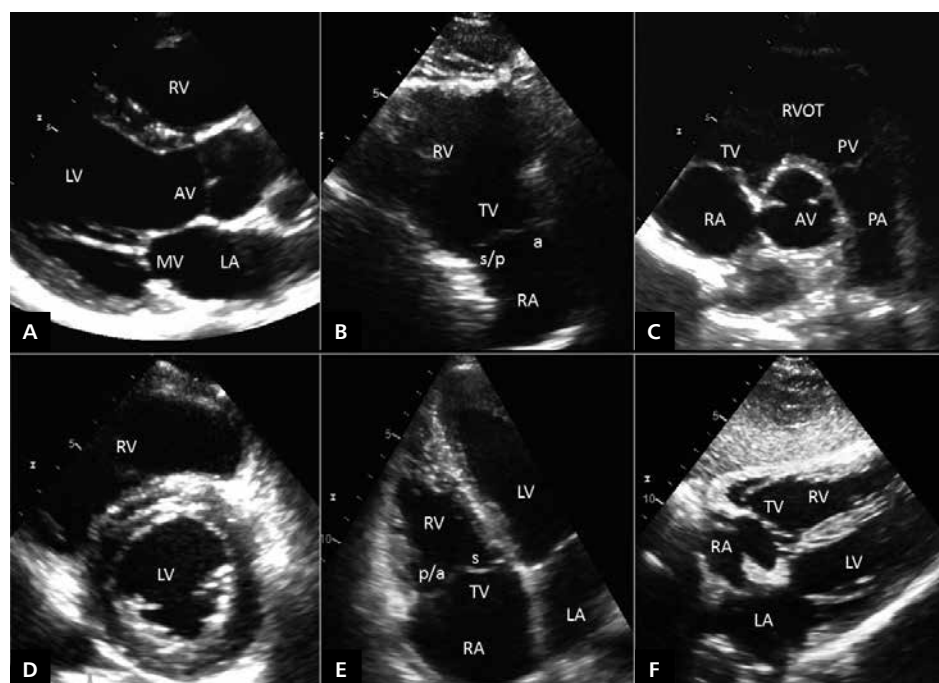


Figure 3. Recommended echocardiographic views for the assessment of the right ventricle (RV); **A.** Parasternal long-axis view demonstrating the RV anterior wall and proximal part of the right ventricular outflow tract (RVOT); **B.** Parasternal long-axis view of RV inflow visualising anterior and inferior walls of the RV, RV inflow tract, and two leaflets of the tricuspid valve (TV) (a — anterior leaflet of TV; p — posterior leaflet of TV; s — septal leaflet of TV); **C.** Parasternal short-axis view of RVOT and pulmonary artery (PA) showing basal part of RV anterior wall, RVOT, two leaflets of the TV, pulmonary valve (PV), and PA; **D.** Parasternal short-axis view at the level of papillary muscles used for the evaluation of the RV crescent shape, calculation of the eccentricity index, and assessment of the interventricular septum motion; **E.** RV-focused apical four-chamber view used to assess the inflow and apical part of the RV, RV lateral wall, interventricular septum, and leaflets of the TV (septal and posterior in the vast majority of patients); **F.** Subcostal four-chamber view visualising the RV inferior wall; AV — aortic valve; LA — left atrium; LV — left ventricle; MV — mitral valve; RA — right atrium

at end systole or during the whole cardiac cycle — for RV pressure overload [6].

Visual assessment of the RV size may be performed from the apical four-chamber view using an approximation that the area of normal RV should not exceed two-thirds of the LV. It is worth noting that this assumption may be misleading in patients with LV dilatation.

Evaluation of the RV walls' structure and motion is clinically important since some pathological conditions are characterised by specific patterns of RV regional contraction. Localised RV dyskinesia or aneurysm is an important diagnostic criterion for arrhythmogenic RV cardiomyopathy (Fig. 5) [10]. Hypokinesia of the RV free wall combined with the normal contraction of the RV apex (McConnell sign) in the presence of RV pressure overload is a typical finding in patients with acute pulmonary embolism [11]. RV wall motion abnormalities can also be seen in patients with RV myocardial infarction, chronic pulmonary hypertension, and congenital heart disease. However, identification of wall motion abnormalities only on the basis of visual echocardiographic assessment may be inaccurate [3].

QUANTITATIVE ASSESSMENT

Right ventricular size

Assessment of RV size by 2DE relies on several dimensions obtained at end-diastole from different echocardiographic views (Table 1). Current guidelines show how to perform the recommended RV linear and area measurements, with RV outflow tract (RVOT) distal diameter being the most reproducible [9, 12]. Despite being easily obtainable and fast, RV diameters may vary significantly with minor rotation or tilting the transducer (Fig. 6) and should be performed only in standard recommended views [12, 13]. The RV areas should be obtained by manual tracing of the RV endocardial border at end diastole and end systole. It is important to ensure that the entire RV including the apex and the free wall is encompassed in the imaging sector during both systole and diastole. While tracing the RV area, the trabeculae must be included in the RV cavity. Normal values for RV 2D linear and area dimensions are listed in Table 1.

The lack of precise anatomic landmarks to define the RV standard views may lead to an under- or overestimation of RV size. Care should be taken to obtain the true

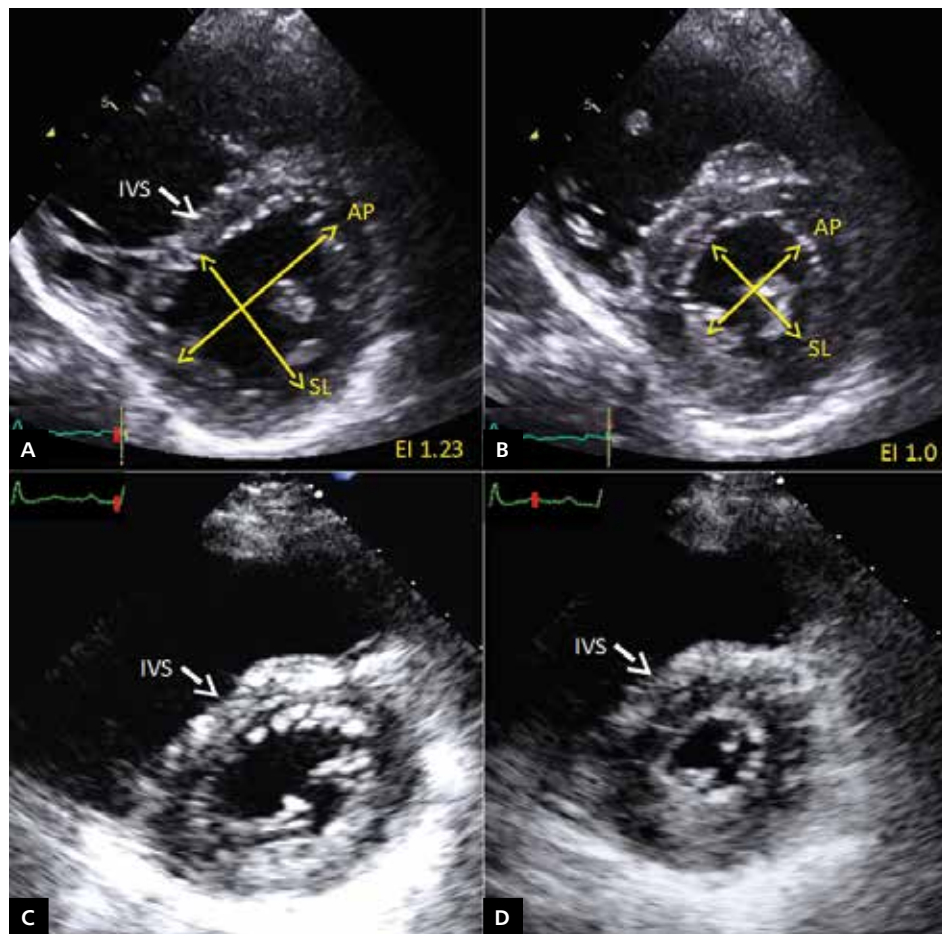


Figure 4. Assessment of the right ventricular (RV) shape and interventricular septum (IVS) motion in parasternal short-axis view at the level of papillary muscles. Stop-frame two-dimensional echocardiography images from a patient with an isolated RV volume overload due to severe tricuspid regurgitation (**A, B**) and from a patient with pressure overload due to primary pulmonary hypertension (**C, D**). In patients with RV volume overload the leftward septal shift and flattening are observed during diastole with left ventricle (LV) taking the shape of the letter 'D' (**A**), whereas a circular profile of LV cavity is maintained during systole (**B**). In patients with RV pressure overload the septal flattening and deformation of the LV are maintained also during systole (**C, D**). Eccentricity index allows the quantitation of the LV shape changes by dividing LV antero-posterior diameter (AP) by septo-lateral diameter (SL), during both systole and diastole. An eccentricity index (EI) value greater than one at end diastole is a strong indicator of RV volume overload (**A**). At end systole or during the whole cardiac cycle it suggests the RV pressure overload

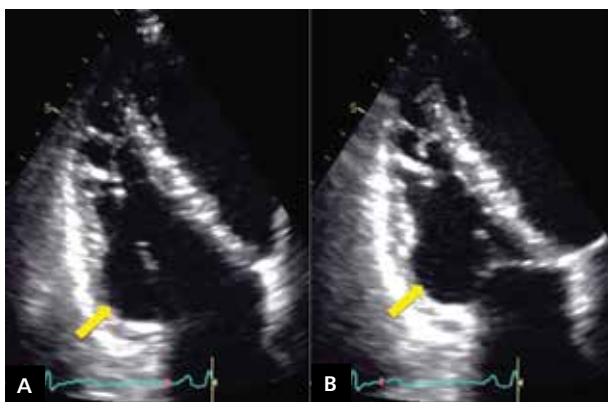


Figure 5. Localised deformation of the basal segment of the right ventricular (RV) lateral wall (arrow) seen in the apical RV-focused four-chamber view both in diastole (**A**) and systole (**B**), due to RV aneurysm in a patient with arrhythmogenic RV cardiomyopathy

Table 1. Normal values for the right ventricle (RV) linear and area dimensions [18]

Dimension	Normal values	Abnormality threshold	Echocardiographic imaging
RV basal diameter [mm]	33 ± 4	> 41	
RV mid diameter [mm]	27 ± 4	> 35	
RVOT proximal diameter [mm]	28 ± 3.5	> 35	
RVOT distal diameter [mm]	22 ± 2.5	> 27	
RV EDA [cm ²]			
Men	17 ± 3.5	> 24	
Women	14 ± 3	> 20	
RV EDA indexed to BSA [cm ² /m ²]			
Men	8.8 ± 1.9	> 12.6	
Women	8.0 ± 1.75	> 11.5	
RV ESA [cm ²]			
Men	9 ± 3	> 15	
Women	7 ± 2	> 11	
RV ESA indexed to BSA [cm ² /m ²]			
Men	4.7 ± 1.35	> 7.4	
Women	4.0 ± 1.2	> 6.4	
RV wall thickness (mm)	3 ± 1	> 5	

BSA — body surface area; EDA — end-diastolic area; ESA — end-systolic area; RVD1 — right ventricular basal diameter; RVD2 — right ventricular mid diameter; RVOT — right ventricular outflow tract

RV-focused four-chamber image with the LV apex at the centre of the scanning sector, while displaying the largest basal RV diameter and thus avoiding foreshortening. The accuracy of RV measurements may be compromised also when the RV free wall is not well defined. Adjusting the gain settings and compression is essential to achieve good image quality. 2DE assessment of the RV appears to be even less accurate in patients with dilated RV, which is common in many pathological settings [14]. Some RV dimensions are of special importance in particular conditions, i.e. the proximal RVOT diameter is useful in the diagnosis of arrhythmogenic RV cardiomyopathy, and the distal RVOT is required for the calculation of Qp/Qs in the presence of intracardiac shunts (Table 1) [9]. In addition to linear and area measurements, RV wall thickness is another parameter routinely measured

by 2DE when assessing the RV geometry. This is particularly important in patients with RV pressure overload, biventricular hypertrophic cardiomyopathies, and storage diseases. It is recommended to use the zoomed image of the RV free wall from subcostal four-chamber view for measurements of its thickness at end diastole in the subtricuspid region because of its higher reproducibility (Fig. 3, Table 1) [9].

Some segments of the RV, such as the outflow tract (contributing up to 25–30% of the RV volume) could be overlooked when using standard 2D transthoracic echocardiography. Transoesophageal echocardiography (TEE) with the mid-oesophageal inflow-outflow view can evaluate RVOT with higher precision [9]. TEE is essential in the peri- and intra-operative settings and allows a continuous monitoring of right heart function during non-cardiac surgery [15]. In addition

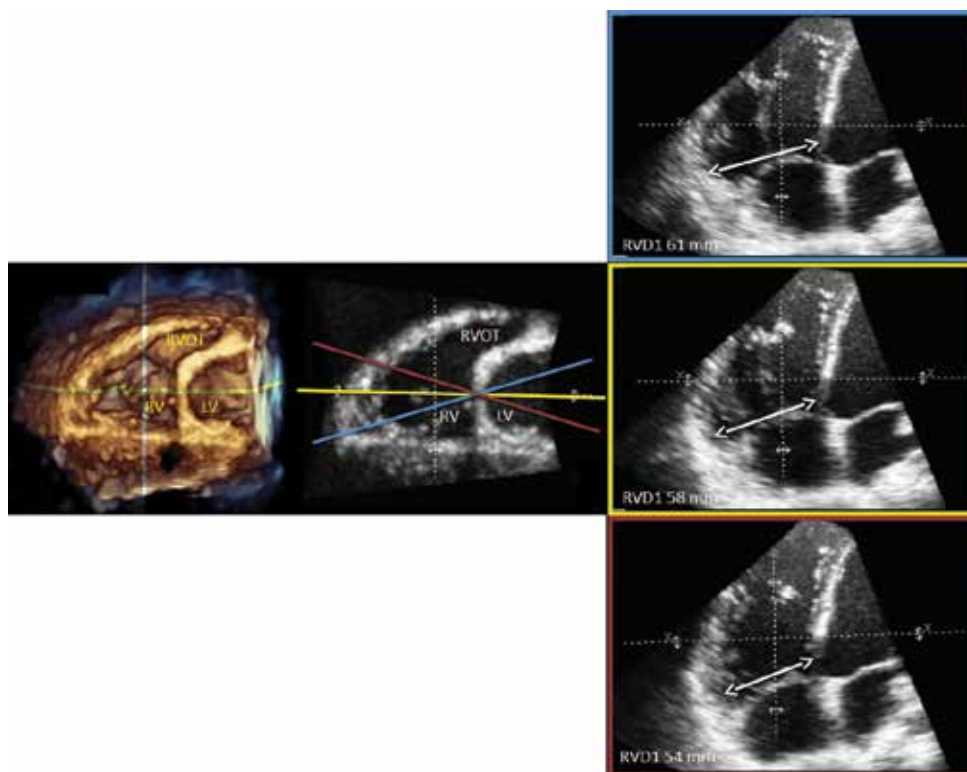


Figure 6. Due to the crescent shape of the right ventricular, minor alterations of the two-dimensional echocardiography apical four-chamber plane orientation shown on the short-axis slices (blue, yellow, and red lines in the central panel) obtained from transversal cut planes of a three-dimensional data set of the right ventricle (RV) seen from the ventricular perspective (left panel) result in significant changes of the RV basal linear dimensions (right panels); LV — left ventricle; RVD1 — right ventricular basal diameter; RVOT — right ventricular outflow tract

to standard TEE views a series of five deep transgastric views have been proposed to obtain additional information on the RV inflow tract, free wall, outflow tract, and the right-sided valves [16]. The current guidelines for the 28-view comprehensive TEE examination incorporate some of these views in order to optimise RV visualisation [17].

Unlike 2DE, 3DE allows multiplane imaging and full volume datasets derived from either a single beat capture or consecutive multibeat narrow angle volumes stitched together with higher temporal and spatial resolution. The 3DE dataset can be analysed using dedicated software packages to obtain the mapping of the RV endocardial surface and the measurements of the RV volumes (Fig. 7). 3DE measurements are closely correlated (but slightly underestimate) with RV volumes measured by CMR both in children and adults [18–21], and by volumetric thermodilution during cardiac catheterisation [22]. Normative data for 3DE RV volumes and ejection fraction (EF) including age-, body size-, and sex-specific reference values based on large cohort studies of healthy volunteers have recently become available (Table 2) [23, 24]. Recent chamber quantification guidelines for the first time included recommendations for 3D analysis of the RV specifying RV

end-diastolic volume of 87 mL/m² in men and 74 mL/m² in women, and RV end-systolic volume of 44 mL/m² in men and 36 mL/m² in women as the upper normal range limits (Table 3) [12].

Three-dimensional echocardiography, however, has specific limitations. 3D volumetric analysis of the RV is highly dependent on image quality, especially on the stage of identification of the endocardial surface in the coronal view required by existing software packages (Fig. 7C). A new methodology for a volumetric analysis of the RV, eliminating the need for extraction of coronal views from a 3D data set, was recently implemented. It proved to be fast and highly reproducible on a large cohort of patients with different RV size and function, and its results correlate well with the CMR [25, 26]. Other important limitations of the technique include, possible drop-out of the RV anterior wall, incomplete visualisation in case of severe dilation, the need for regular heart rate, and patients' cooperation. Nevertheless, specific advantages of 3DE over other modern imaging modalities, including its portability, absence of ionising radiation, and the ability to examine patients with pacemakers and defibrillators, make 3DE one of the most versatile and important techniques to assess the RV.

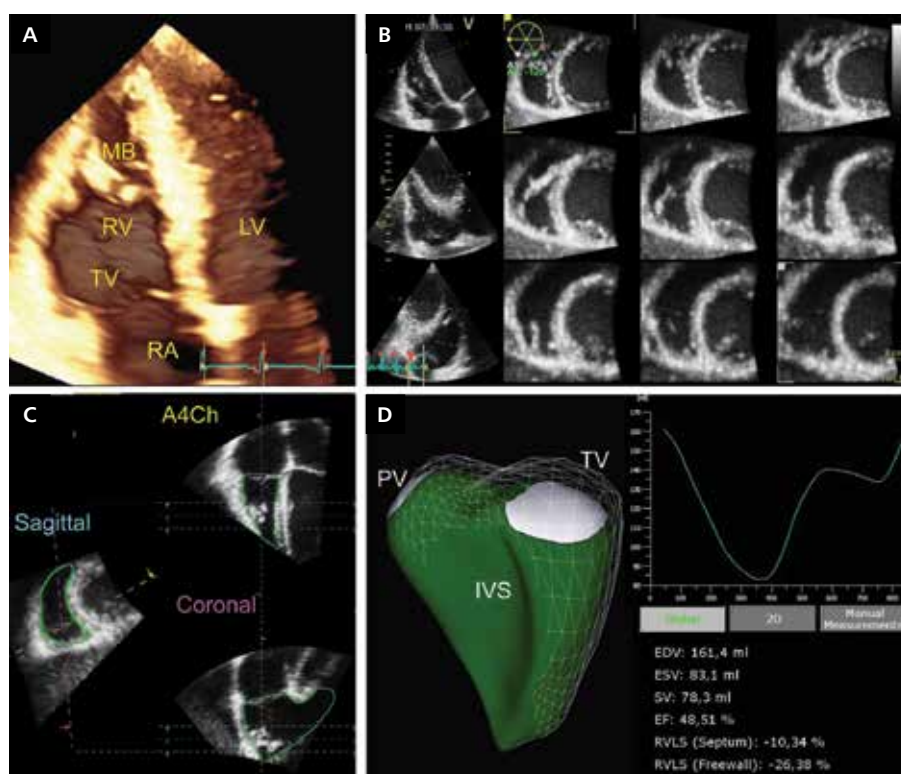


Figure 7. Display modes of a three-dimensional (3D) data set of the right ventricle (RV) obtained from the RV-focused apical four-chamber view using full-volume multi-beat acquisition (four to six consecutive beats) with adjusted depth and volume width to encompass the entire RV; **A.** Volume rendering demonstrating the RV anatomy; **B.** Multi (twelve)-slice mode including three longitudinal (0° , 60° , and 120°) and nine transversal equidistant tomographic views between the apex and the base of the RV, mainly used for regional wall motion and RV shape analysis; **C.** Semiautomatic identification of the RV endocardial surface in the RV short-axis, four-chamber, and coronal views; **D.** Surface rendered 3D model of the RV (green model) combining the wire-frame (white cage) display of the end-diastolic volume. Surface-rendered dynamic model changes its size and shape throughout the cardiac cycle enabling the visual assessment of the RV dynamics and quantitation of RV volumes and ejection fraction; EDV — end-diastolic volume; EF — ejection fraction; ESV — end-systolic volume; IVS — interventricular septum; LV — left ventricle; MB — moderator band; PV — pulmonic valve; RA — right atrium; RVLS — right ventricular longitudinal strain; SV — stroke volume; TV — tricuspid valve

Table 2. Principal studies of three-dimensional echocardiography (3DE) reference values for the right ventricle (RV) volumes and ejection fraction in adult healthy volunteers

	Maffessanti F., 2013 [24]		Tamborini G., 2010 [23]	
	Male	Female	Male	Female
Population size	247	260	119	126
Population type	Healthy adult volunteers		Healthy adult volunteers	
Age [years]	45 ± 16		48 ± 17	
End-diastolic volume [mL]	107 (74, 163)	81 (58, 120)	99 ± 14	74 ± 14
EDVi [mL/m ²]			52 ± 8	46 ± 8
End-systolic volume [mL]	44 (22, 80)	30 (15, 52)	35 ± 7	23 ± 7
ESVi [mL/m ²]			18 ± 4	14 ± 4
Ejection fraction [%]	60 (45, 75)	63 (49, 79)	64 ± 8	69 ± 8
Study limitations	<ul style="list-style-type: none"> • No comparison between RV parameters obtained by 3DE and CMR. • The RV values in patients ≥ 70 years (males in particular) should be interpreted with caution, given the small size of this age group. 			

Data are expressed as mean ± standard deviation or median (5th, 95th percentile); CMR — cardiac magnetic resonance; EDVi — index of end-diastolic volume; ESVi — index of end-systolic volume

Table 3. Normal values for the right ventricle volumes and ejection fraction obtained by three-dimensional echocardiography [18]

Dimension	Normal values	Abnormality threshold
Index of end-diastolic volume [mL/m ²]		
Men	61 ± 13	> 87
Women	53 ± 10.5	> 74
Index of end-systolic volume [mL/m ²]		
Men	27 ± 8.5	> 44
Women	22 ± 7	> 36
Ejection fraction [%]	58 ± 6.5	< 45

RIGHT VENTRICULAR FUNCTION

Right ventricular systolic function

The RVEF is an independent predictor of cardiovascular morbidity and mortality in various conditions [2, 27]. The assessment of RVEF using 2DE is no longer recommended due to its inaccuracy [9, 12]. In the absence of a single reliable measure of the RV systolic function using conventional echocardiography, a number of surrogate echocardiographic parameters (RV fractional area change, tricuspid annular plane systolic excursion, peak S wave velocity of the lateral tricuspid annulus by tissue Doppler imaging [TDI], and RV myocardial performance index) have been proposed for clinical use (Table 4). However, it is worth stressing that only RVEF provides an adequate assessment of true global RV pump function, and 3DE remains the only echocardiographic technique capable of a reliable calculation of RVEF from end-diastolic and end-systolic volume measurements (Fig. 7D). Recent studies have confirmed that 3DE measurements of the RVEF are accurate, reproducible, and correlate well with CMR both in adults and children [20, 21, 27, 28]. In the most recent meta-analysis aimed at exploring the accuracy of different imaging modalities (2DE, 3DE, radionuclide ventriculography, computed tomography [CT], gated single-photon emission CT, and invasive cardiac cineventriculography) for RVEF using CMR as a reference method, 3DE has proven to be the most reliable technique, overestimating the RVEF by only 1.16% with the lowest limits of agreement (from -0.59 to 2.92%) [29]. Importantly, due to the architecture of the RV, RVEF is particularly sensitive to RV loading conditions and cannot be considered a reliable parameter of RV myocardial contractility in patients with significant RV volume- or pressure overload. The reference values of 3DE RVEF have recently been obtained on large cohorts of healthy volunteers (Table 2) [23, 24], and reports on performance in disease conditions are accumulating [30]. Importantly, recent guidelines suggest that in laboratories with appropriate 3D platforms and experience 3DE-derived RVEF should be considered a method of choice for quantifying

RV systolic function, with the abnormality threshold < 45% (Table 3) [12]. Guideline documents regarding 3DE image acquisition and display have been published [31].

Right ventricular diastolic function

Although the evaluation of RV diastolic function is rarely considered a part of routine echo examination, it can provide valuable diagnostic information. During acute RV pressure overload, RV diastolic function is not affected, whereas chronic RV pressure overload impacts RV diastolic dysfunction, resulting in prolonged diastolic relaxation time and increased RV diastolic stiffness [32]. The assessment of RV diastolic function includes the evaluation of the RV inflow by pulsed wave Doppler sampling at the tips of the tricuspid valve leaflets; measuring the TDI velocities of the tricuspid annulus at RV free wall; evaluation of right atrial, inferior vena cava, and hepatic vein size and function. Although preload-dependent, the tricuspid E/e' ratio is a good marker of RV diastolic dysfunction in pulmonary hypertension and an indicator of RV filling pressure; E/e' values > 6 have a sensitivity of 79% and a specificity of 73% for the detection of right atrial pressure > 10 mm Hg. The following grading of RV diastolic dysfunction has been suggested: tricuspid E/A < 0.8 suggests impaired relaxation, a tricuspid E/A of 0.8 to 2.1 with an E/e' > 6 or diastolic flow predominance in the hepatic veins suggests pseudonormal filling, and a tricuspid E/A > 2.1 with a deceleration time < 120 ms suggests restrictive filling [9].

The data about the impact of RV diastolic dysfunction on patients' outcome are scarce. It was demonstrated that patients with left-sided heart failure and RV diastolic dysfunction defined by abnormal filling profiles have an increased risk of unstable angina and hospital readmissions due to heart failure deterioration [33].

Right ventricular mechanics

Being extremely load dependent, RVEF is a partial indicator of the RV systolic function, which is the result of complex myocardial mechanics as discussed in the paragraph dedicated to RV anatomy and physiology. Myocardial deformation imaging is a relatively novel echocardiographic technique that allows the evaluation of RV myocardial mechanics. The clinical and prognostic value of the RV strain was demonstrated in patients with pulmonary hypertension, heart failure and LV assist devices, congenital heart diseases, storage diseases, and cardiomyopathies with high risk of malignant ventricular arrhythmias [34–36]. Echocardiographic assessment of RV myocardial deformation can be performed using either TDI or 2DSTE techniques (Fig. 8) [37]. The correlation between Doppler-derived and 2DSTE-derived RV longitudinal strain appears to be moderate; however, both techniques are considered feasible and accurate enough to differentiate between physiological and pathological conditions [38].

Table 4. Normal values for conventional echocardiographic parameters in assessing systolic function of the right ventricle (RV) [18]

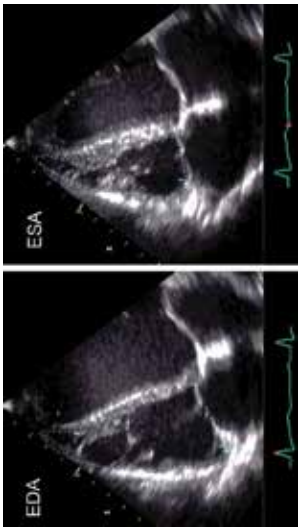

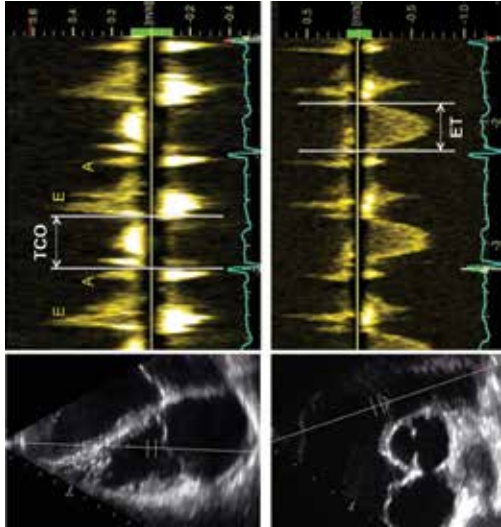
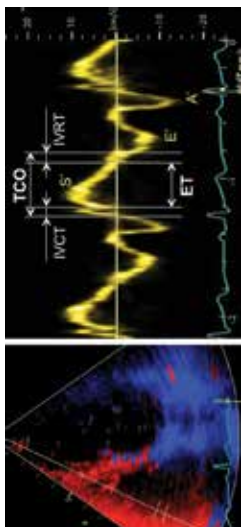
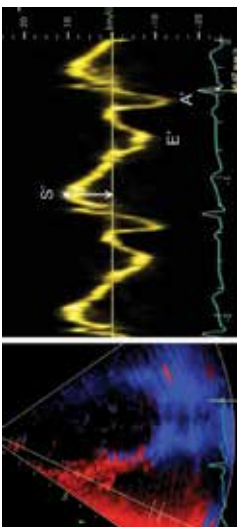
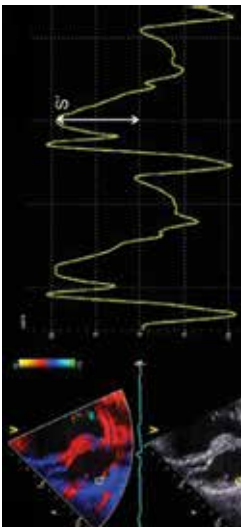
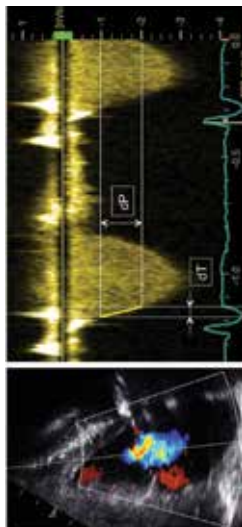
Parameter	Normal values	Advantages	Limitations	Essential for correct use	Echocardiographic imaging
FAC [%]	49 ± 7	Reflects both longitudinal and radial components of RV contraction Established prognostic values Correlates with RV EF by CMR	Requires good endocardial border delineation Neglects the contribution of RVOT to overall systolic function Only fair inter-observer reproducibility Affected by the overall heart motion (not recommended after cardiac surgery)	Sufficient image quality (endocardial delineation) Four-chamber RV-focused view	 <p>FAC = (EDA + ESA)/EDA</p>
TAPSE [mm]	24 ± 3.5	Easy to obtain Less dependent on image quality Established prognostic value	Reflects only the longitudinal function Neglects the contribution of the IVS and the RVOT Angle dependency	Good alignment	
Pulsed Doppler RIMP	0.26 ± 0.085	Established prognostic value	Requires matching for R-R intervals when measurements are performed on separate recordings Unreliable when RA pressure is elevated Limited use in normal RV	Regular heart rhythm Sufficient Doppler signal	 <p>RIMP = (TCO - ET)/ET</p>

Table 4. cont. Normal values for conventional echocardiographic parameters in assessing systolic function of the right ventricle (RV) [18]

Tissue Doppler RIMP	0.38 ± 0.08	Less affected by heart rate Single-beat recording with no need for R-R interval matching	Unreliable when RA pressure is elevated	Good alignment	 $RIMP = (TCO - ET)/ET = (IVRT + IVCT)/ET$
Pulsed tissue Doppler S' wave [cm/s]	14.1 ± 2.3	Easy to perform Reproducible Validated against radionuclide EF Established prognostic value	Angle dependent Load-dependent Influenced by TR Not fully representative of RV global function, particularly after cardiac surgery	Good alignment	
Colour tissue Doppler S wave [cm/s]	9.7 ± 1.85	Allows multisite sampling on the same beat May be also used for assessment or the RV dyssynchrony by time delay between RV free wall and IVS	Requires postprocessing Angle dependent Not fully representative of RV global function, particularly after cardiac surgery	Sufficient image quality of RV free wall	
dP/dT [mm Hg/s]	Abnormality threshold < 400 mm Hg/s	Easy to obtain	Load-dependent Unreliable in severe TR Inapplicable in patients with no/minimal TR	Sufficient TR continuous-wave Doppler signal	

CMR — cardiac magnetic resonance; EF — ejection fraction; EDA — end-diastolic area; ESA — end-systolic area; ET — ejection time; FAC — fractional area change; IVRT — isovolumic relaxation time; IVCT — isovolumic contraction time; IVS — interventricular septum, RA — right atrium; RIMP — right atrium; RIMP — right ventricular index of myocardial performance; RVOT — right ventricular outflow tract; TAPSE — tricuspid annulus peak systolic velocity; TCO — tricuspid valve closure-to-opening time; TR — tricuspid regurgitation

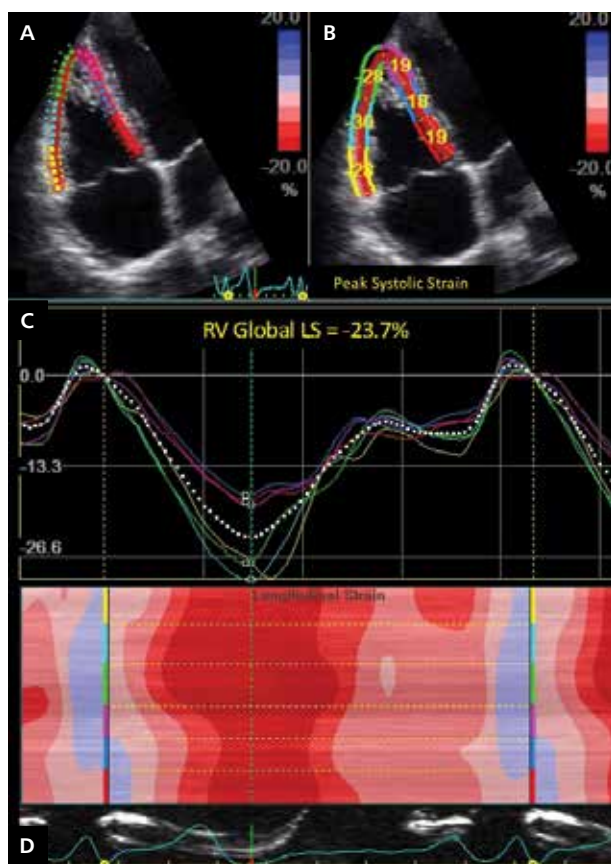


Figure 8. Peak systolic longitudinal strain (LS) of the right ventricular (RV) free wall and interventricular septum obtained with two-dimensional speckle-tracking analysis; **A.** Parametric colour-coded display of end-systolic strain; **B.** Regional end-systolic strain; **C.** Strain-time curves. Coloured curves show the segmental strain change during the cardiac cycle, and white dotted line shows the global RV strain changes during the cardiac cycle; **D.** Anatomical M-mode colour-coded display of segmental strain variations during the cardiac cycle

Although strain calculations from TDI do not rely on specific geometrical assumptions, a number of issues, including angle-dependence of the Doppler technique, thin myocardial wall with large systolic longitudinal and transversal excursion, need for high frame rates, and drifting of the strain curve, as well as the influence of age and heart rate, significantly affect the accuracy and reproducibility of strain and strain rate measurements with TDI. Conversely, 2DSTE is an angle-independent technique but it relies more on the image quality than on TDI. Both techniques are mostly limited to the apical four-chamber view and evaluate only RV longitudinal strain.

The normative data for the RV strain were mostly obtained from small cohorts of adults representing the control groups in pathologic studies [9]. In the most up-to-date version of the chamber quantification guidelines an abnormality threshold for the RV free-wall longitudinal strain was set at -20% [12]. In a recent prospective study performed

on 116 subjects free from cardiopulmonary disease and/or risk factors, the mean free wall longitudinal systolic RV strain value was $-26 \pm 4\%$, which is in agreement with the value of $-27 \pm 2\%$ obtained in a meta-analysis of 10 studies involving 486 healthy individuals [39]. There is a need in normative values of longitudinal strain for separate segments of the RV because the information on a regional strain impairment may play an important role in diagnosis of specific RV pathology, such as arrhythmogenic RV cardiomyopathy. In addition to the lack of reference values, the major limitations of 2DSTE longitudinal strain of the RV include the loss of speckles due to excessive motion of RV lateral wall, inter-vendor variability, and the lack of standardisation in the measurement and reporting of strain parameters [39, 40].

Although “global” RV longitudinal strain is supposed to represent the longitudinal deformation of the whole RV, none of the currently available algorithms is capable of providing such information. The term “global” RV longitudinal strain is commonly used for average values calculated from three segments of the RV free wall and three segments of the IVS from apical four-chamber view, even though the contribution of other walls and RVOT is neglected. Inconsistent use of this term in some studies (denoting average strain of six segments [41], or three RV free wall segments alone [42]) may be misleading because these methodologies return different results. Many studies reported only free wall RV longitudinal strain, therefore providing information on a very limited part of the RV and its contribution to systolic performance. Similarly, there is no consensus whether RV strain should be obtained as the mean strain from the averaged strain curve of all segments or the mean peak systolic strain calculated by averaging the peak segmental values. In a recent study of healthy individuals, the authors recommended use of a six-segment approach on the apical four-chamber RV-focused view as a more robust analysis method, and computation of the RV free wall longitudinal strain by averaging the peak segmental values displayed by the software [43]. Reference values for RV strain with and without including the IVS are listed in Table 5.

The determination of circumferential shortening requires short-axis views of RV, which are hardly obtainable by 2DE, and data on its potential role in clinical management is limited. The possibility of obtaining the RV free wall circumferential strain from the subcostal LV short-axis view was demonstrated in a group of children with RV pressure overload. It provided better information about RV function, and correlated significantly more with RVEF and RV systolic pressure obtained by cardiac catheterisation than global RV longitudinal strain [44].

The development of 3DE enabled the echocardiographic assessment of RV mechanics in various directions (i.e. longitudinal, circumferential and area strain, a combination of longitudinal and circumferential shortening), similar to CMR. Good inter- and intra-observer reproducibility was

Table 5. Reference values of the right ventricular longitudinal strain (RVLS) in the overall study population and separated by gender [68]

Strain parameters	Overall	Men	Women	P*
Global six segments RVLS				
Average (%)	-25.7 [-23.5; -28.1]	-24.5 [-22.6; -26.3]	-26.6 [-24.5; -28.5]	< 0.001
Free wall three segments RVLS				
Average (%)	-30.6 [-27.7; -33.0]	-29.3 [-27.0; -31.9]	-31.8 [-29.3; -33.9]	< 0.001
Basal (%)	-30.0 [-26.0; -35.0] ^	-28.0 [-25.0; -33.0] ^	-31.0 [-27.0; -37.0] ^	0.002
Mid (%)	-34.0 [-30.0; -37.8]	-32.0 [-29.0; -35.0]	-35.0 [-32.0; -40.0]	0.001
Apex (%)	-28.5 [-25.0; -32.0] ^	-27.0 [-25.0; -30.0] ^	-30.0 [-26.0; -33.0] ^	< 0.001
Septal three segment RVLS				
Average (%)	-20.0 [-18.0; -22.0]	-19.0 [-17.3; -21.7]	-20.3 [-18.9; -22.4]	0.012
Basal (%)	-20.0 [-18.0; -22.0] ^	-19.0 [-17.0; -22.0] ^	-20.0 [-18.0; -23.0] ^	0.002
Mid (%)	-20.0 [-19.0; -22.0]	-20.0 [-18.0; -22.0]	-21.0 [-19.0; -23.0]	0.001
Apex (%)	-20.0 [-17.00; -23.0] ^	-19.0 [-15.0; -23.0] ^	-20.0 [-17.0; -24.0] ^	0.017

Data represent median [I, III quartile]; *Men vs. women; ^ p < 0.05 for mid vs. basal or mid vs. apex

demonstrated in a heterogeneous group of patients for all the measurements of 3D RV mechanics (correlation coefficients 0.7–0.9) [45]. Area strain correlated with RVEF and was a strong predictor of death, suggesting the superiority of 3DE-derived area strain over other deformation parameters [46]. Whether 3DE-derived strain has an added value in routine assessment of RV remains unclear, given the fact that only small populations have been investigated to date and normal values are yet to be established.

RIGHT VENTRICULAR DYSSYNCHRONY

In addition to quantification of regional RV systolic function and myocardial mechanics, strain and strain-rate can be used for the assessment of RV dyssynchrony, a new promising approach to the evaluation of RV dysfunction in patients with different cardiac conditions. Interventricular and RV intra-ventricular dyssynchrony have been described in pulmonary artery hypertension showing strong correlation of RV dyssynchrony indexes with the extent of RV dysfunction, pulmonary artery pressure, and adverse RV remodelling [47, 48]. Due to the complexity of the RV geometry the assessment of its dyssynchrony is only feasible by measuring IVS — RV free wall delay obtained by TDI or 2DSTE algorithms (Fig. 9). The cut-off values to identify RV intra-ventricular dyssynchrony were described in a small cohort of healthy individuals and calculated as the standard deviation of the time to peak-systolic strain for the mid and basal RV segments corrected to the R-R interval. Using the upper 95% limit of normal range a cutoff value of 18 ms was introduced as a criterion for RV dyssynchrony [49]. It was also demonstrated that being an independent predictor of unfavourable prognosis in patients with pulmonary hypertension, RV dyssynchrony might regress as a result of effective therapy. For better understanding of the role of RV dyssynchrony as a biomarker of treatment success

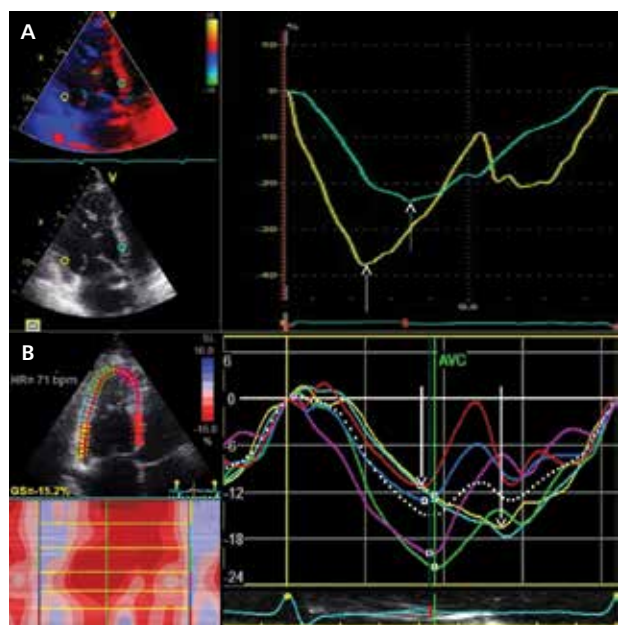


Figure 9. Measurement of the right ventricular (RV) dyssynchrony; **A.** Tissue Doppler pulsed-wave Doppler algorithm for assessment of RV dyssynchrony based on the difference between time-to-peak strain of the basal segments of inter-ventricular septum (IVS) and free wall of the RV in apical four-chamber view (arrows indicate peak systolic strain); **B.** Peak systolic longitudinal strain of the RV free wall and IVS obtained with two-dimensional speckle-tracking. The coloured lines represent the time-interval between QRS onset and peak systolic strain for each RV segment for dyssynchrony measurement. Arrows indicate the peak systolic strain of basal lateral (yellow curve) and basal septal (red curve) segments; AVC — aortic valve closure

and predictor of survival, these findings should be confirmed in larger studies.

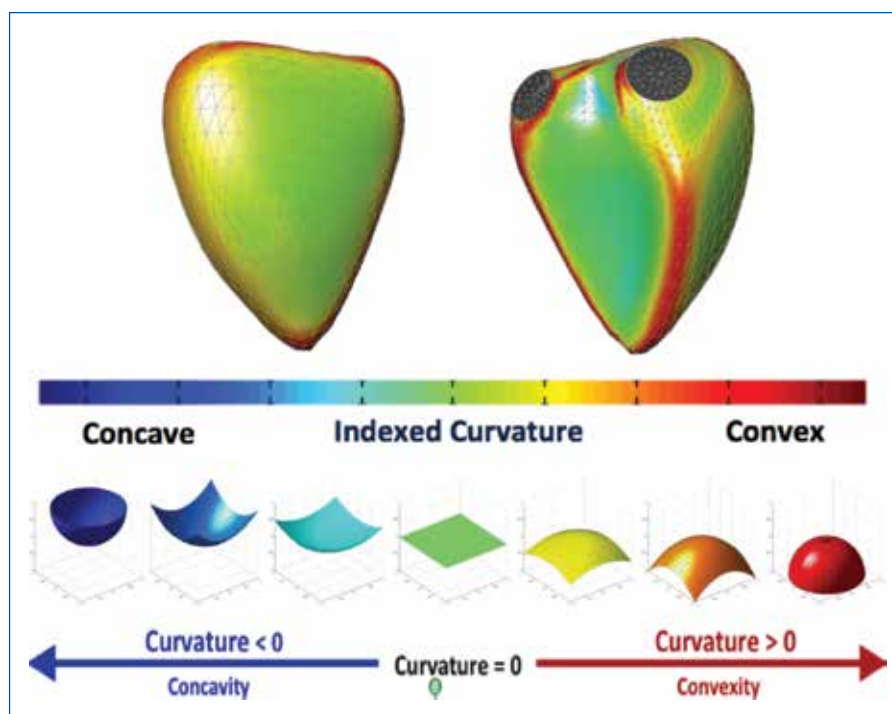


Figure 10. Three-dimensional (3D) echocardiography-based analysis of right ventricular (RV) shape. To quantify RV shape the 3D endocardial surface of RV was divided into six regions. For each node in a given region, two values were analytically derived: 1) the maximum curvature k_1 — the inverse of the radius of the smallest circle fitting the surface at that particular node (r_1) and 2) the curvature k_2 — the inverse radius of the fitting circle (r_2) in the perpendicular direction. The mean 3D curvature k was obtained by averaging the two values k_1 and k_2 for each point of the mesh. Each node was normalised by the curvature of the sphere having the same volume as the whole ventricle. This last step accounts for changes in curvature due to changes in RV volume. For the purpose of curvature visualisation, the 3D endocardial surface was colour-coded to depict local 3D curvature values; zero = flat surface. Positive signifies convexity and negative signifies concavity. (Courtesy of Dr. Karima Addettia)

RIGHT VENTRICULAR SHAPE

Unlike the LV, data on RV remodelling and shape alterations are scarce. The complex shape of the RV cannot be simplified to a spherical or bullet-like morphology, which is why its assessment is challenging even in normal individuals. From a mechanical perspective, the RV wall stress was shown to be a major factor in RV failure development [50]. However, for a long time there was no evidence supporting poor outcomes or increased mortality in patients with adverse RV shape changes independent of that predicted by size and functional parameters.

A methodology that allows the assessment of 3DE-derived global and regional RV shape indices based on analysis of the RV curvature was recently developed and tested in normal subjects and in patients with pulmonary arterial hypertension (Fig. 10) [51]. It was demonstrated that in patients with pressure overload the RVOT is more round and both body and apical portions of the septum are more convex, bulging into the LV at both end-diastole and end-systole, with a more flattened apical free wall. The curvature of the RV inflow tract was a more robust predictor of death than RVEF, RV volumes, or other regional curvature indices. This promising

methodology could potentially be used for a more effective assessment of the RV and might be useful as a biomarker of a treatment response. Future studies are needed to provide more data on the diagnostic and prognostic role of the RV shape in different clinical settings.

CONCLUSIONS

Right ventricular function and mechanics have proven to be important indicators of overall cardiac function and strong predictors of cardiovascular morbidity and mortality. However, accurate evaluation of the RV geometry and performance with conventional echocardiography remains challenging due to existing limitations of this imaging modality. Recent developments in echocardiographic imaging techniques such as 3DE and speckle-tracking enable more accurate, reproducible, and safe assessment of the RV morphology and functions. Combined results and collective evidence generated using different echocardiographic techniques will provide deeper insights into the pathology of this intriguing cardiac chamber, ultimately translating into more accurate diagnosis and better clinical management of cardiovascular patients.

Conflict of interest: none declared

References

- Haddad F, Doyle R, Murphy DJ et al. Right ventricular function in cardiovascular disease, part II: pathophysiology, clinical importance, and management of right ventricular failure. *Circulation*, 2008; 117: 1717–1731. doi:10.1161/CIRCULATIONAHA.107.653584.
- Murninkas D, Alba AC, Delgado D et al. Right ventricular function and prognosis in stable heart failure patients. *J Card Fail*, 2014; 20: 343–349. doi: 10.1016/j.cardfail.2014.01.018.
- Buechel ERV, Mertens LL. Imaging the right heart: the use of integrated multimodality imaging. *Eur Heart J*, 2012; 33: 949–960. doi: 10.1093/eurheartj/ehr490.
- Haddad F, Hunt SA, Rosenthal DN et al. Right ventricular function in cardiovascular disease, part I: Anatomy, physiology, aging, and functional assessment of the right ventricle. *Circulation*, 2008; 117: 1436–1448. doi: 10.1161/CIRCULATIONAHA.107.653576.
- Badano LP, Ghingina C, Easaw J et al. Right ventricle in pulmonary arterial hypertension: haemodynamics, structural changes, imaging, and proposal of a study protocol aimed to assess remodelling and treatment effects. *Eur J Echocardiogr*, 2010; 11: 27–37. doi: 10.1093/ejehocardiography/jep152.
- Jurcut R, Giusca S, La Gerche A et al. The echocardiographic assessment of the right ventricle: What to do in 2010? *Eur J Echocardiogr*, 2010; 11: 81–96. doi: 10.1093/ejehocardiography/jep234.
- Friedberg MK, Redington AN. Right versus left ventricular failure: differences, similarities, and interactions. *Circulation*, 2014; 129: 1033–1044. doi: 10.1161/CIRCULATIONAHA.113.001375.
- Sheehan F, Redington A. The right ventricle: anatomy, physiology and clinical imaging. *Heart*, 2008; 94: 1510–1515. doi: 10.1136/hrt.2007.132779.
- Rudski LG, Lai WW, Afilalo J et al. Guidelines for the echocardiographic assessment of the right heart in adults: a report from the American Society of Echocardiography endorsed by the European Association of Echocardiography, a registered branch of the European Society of Cardiology. *J Am Soc Echocardiogr*, 2010; 23: 685–713. doi: 10.1016/j.echo.2010.05.010.
- Te Riele ASJM, Tandri H, Sanborn DM et al. Noninvasive Multimodality Imaging in ARVD/C. *J Am Coll Cardiol Cardiovasc Imaging*, 2015; 8: 597–611. doi: 10.1016/j.jcmg.2015.02.007.
- Konstantinides SV, Torbicki A, Agnelli G et al. 2014 ESC guidelines on the diagnosis and management of acute pulmonary embolism. *Eur Heart J*, 2014; 35: 3033–3069. doi: 10.1093/eurheartj/ehu283.
- Lang RM, Badano LP, Mor-Avi V et al. Recommendations for cardiac chamber quantification by echocardiography in adults: an update from the American Society of Echocardiography and the European Association of Cardiovascular Imaging. *J Am Soc Echocardiogr*, 2015; 28:1–39.e14. doi: 10.1016/j.echo.2014.10.003.
- Portnoy SG, Rudski LG. Echocardiographic evaluation of the right ventricle: a 2014 perspective. *Curr Cardiol Rep*, 2015; 17: 21. doi: 10.1007/s11886-015-0578-8.
- Lai WW, Gauvreau K, Rivera ES et al. Accuracy of guideline recommendations for two-dimensional quantification of the right ventricle by echocardiography. *Int J Cardiovasc Imaging* 2008; 24: 691–698. doi:10.1007/s10554-008-9314-4.
- Tan CO, Harley I. Perioperative transesophageal echocardiographic assessment of the right heart and associated structures: a comprehensive update and technical report. *J Cardiothorac Vasc Anesth*, 2014; 28:1112–1133. doi: 10.1053/j.jvca.2013.05.031.
- Kasper J, Bolliger D, Skarvan K et al. Additional cross-sectional transesophageal echocardiography views improve perioperative right heart assessment. *Anesthesiology*, 2012; 117: 726–734. doi: 10.1097/ALN.0b013e318269054b.
- Hahn RT, Abraham T, Adams MS et al. Guidelines for performing a comprehensive transesophageal echocardiographic examination: recommendations from the American Society of Echocardiography and the Society of Cardiovascular Anesthesiologists. *Anesth Analg*, 2014; 118: 21–68. doi: 10.1213/ANE.0000000000000016.
- Leibundgut G, Rohner A, Grize L et al. Dynamic assessment of right ventricular volumes and function by real-time three-dimensional echocardiography: a comparison study with magnetic resonance imaging in 100 adult patients. *J Am Soc Echocardiogr*, 2010; 23: 116–126. doi: 10.1016/j.echo.2009.11.016.
- Gopal AS, Chukwu EO, Iwuchukwu CJ et al. Normal values of right ventricular size and function by real-time 3-dimensional echocardiography: comparison with cardiac magnetic resonance imaging. *J Am Soc Echocardiogr*, 2007; 20: 445–455. doi: 10.1016/j.echo.2006.10.027.
- Lu X, Nadvoretzkiy V, Bu L et al. Accuracy and reproducibility of real-time three-dimensional echocardiography for assessment of right ventricular volumes and ejection fraction in children. *J Am Soc Echocardiogr*, 2008; 21: 84–89. doi: 10.1016/j.echo.2007.05.009.
- Bin Zhang Q, Sun JP, Gao RF et al. Feasibility of single-beat full-volume capture real-time three-dimensional echocardiography for quantification of right ventricular volume: validation by cardiac magnetic resonance imaging. *Int J Cardiol*, 2013; 168: 3991–3995. doi: 10.1016/j.ijcard.2013.06.088.
- De Simone R, Wolf I, Mottl-Link S et al. Intraoperative assessment of right ventricular volume and function. *Eur J Cardiothorac Surg*, 2005; 27: 988–993. doi: 10.1016/j.ejcts.2005.01.022.
- Tamborini G, Marsan NA, Gripari P et al. Reference values for right ventricular volumes and ejection fraction with real-time three-dimensional echocardiography: evaluation in a large series of normal subjects. *J Am Soc Echocardiogr*, 2010; 23: 109–115. doi: 10.1016/j.echo.2009.11.026.
- Maffessanti F, Muraru D, Esposito R et al. Age-, body size-, and sex-specific reference values for right ventricular volumes and ejection fraction by three-dimensional echocardiography: a multicenter echocardiographic study in 507 healthy volunteers. *Circ Cardiovasc Imaging*, 2013; 6: 700–710. doi: 10.1161/CIRCIMAGING.113.000706.
- Muraru D, Spadotto V, Cecchetto A et al. New speckle-tracking algorithm for right ventricular volume analysis from three-dimensional echocardiographic datasets: validation with cardiac magnetic resonance and comparison with the previous analysis tool. *Eur Heart J Cardiovasc Imaging*, 2015; Dec 8. doi:10.1093/ehjci/jev309.
- Medvedofsky D, Addetia K, Patel AR et al. Novel approach to three-dimensional echocardiographic quantification of right ventricular volumes and function from focused views. *J Am Soc Echocardiogr*, 2015; 28: 1222–1231. doi: 10.1016/j.echo.2015.06.013.
- Sugeng L, Mor-Avi V, Weinert L et al. Multimodality comparison of quantitative volumetric analysis of the right ventricle. *J Am Coll Cardiol Cardiovasc Imaging*, 2010; 3: 10–18. doi: 10.1016/j.jcmg.2009.09.017.
- Niemann PS, Pinho L, Balbach T et al. Anatomically oriented right ventricular volume measurements with dynamic three-dimensional echocardiography validated by 3-Tesla magnetic resonance imaging. *J Am Coll Cardiol*, 2007; 50: 1668–1676. doi: 10.1016/j.jacc.2007.07.031.
- Pickett CA, Cheezum MK, Kassop D et al. Accuracy of cardiac CT, radionuclide and invasive ventriculography, two- and three-dimensional echocardiography, and SPECT for left and right ventricular ejection fraction compared with cardiac MRI: a meta-analysis. *Eur Heart J Cardiovasc Imaging*, 2015; 16: 848–852. doi: 10.1093/ehjci/jeu313.
- Kidawa M, Chizyński K, Zielińska M et al. Real-time 3D echocardiography and tissue Doppler echocardiography in the assessment of right ventricle systolic function in patients with

- right ventricular myocardial infarction. *Eur Heart J Cardiovasc Imaging*, 2013; 14: 1002–1009. doi: [10.1093/ehjci/jes321](https://doi.org/10.1093/ehjci/jes321).
31. Lang RM, Badano LP, Tsang W et al. EAE/ASE Recommendations for image acquisition and display using three-dimensional echocardiography. *Eur Heart J Cardiovasc Imaging*, 2012; 13: 1–46. doi: [10.1093/ehjci/jer316](https://doi.org/10.1093/ehjci/jer316).
 32. Gaynor SL, Maniar HS, Bloch JB et al. Right atrial and ventricular adaptation to chronic right ventricular pressure overload. *Circulation*, 2005; 112: I212–I218.
 33. Yu HC, Sanderson JE. Different prognostic significance of right and left ventricular diastolic dysfunction in heart failure. *Clin Cardiol*, 1999; 22: 504–512.
 34. Hardegree EL, Sachdev A, Villarraga HR et al. Role of serial quantitative assessment of right ventricular function by strain in pulmonary arterial hypertension. *Am J Cardiol*, 2013; 111: 143–148. doi: [10.1016/j.amjcard.2012.08.061](https://doi.org/10.1016/j.amjcard.2012.08.061).
 35. Hayek S, Sims DB, Markham DW et al. Assessment of right ventricular function in left ventricular assist device candidates. *Circ Cardiovasc Imaging*, 2014; 7: 379–389. doi: [10.1161/CIRCIMAGING.113.001127](https://doi.org/10.1161/CIRCIMAGING.113.001127).
 36. Lisi M, Cameli M, Righini FM et al. RV longitudinal deformation correlates with myocardial fibrosis in patients with end-stage heart failure. *J Am Coll Cardiol Cardiovasc Imaging*, 2015; 8: 514–522. doi: [10.1016/j.jcmg.2014.12.026](https://doi.org/10.1016/j.jcmg.2014.12.026).
 37. Szymczyk E, Lipiec P, Michalski B, Kasprzak JD. 2D and 3D speckle tracking echocardiography: clinical application. *Kardiol Pol*, 2013; 71: 77–83.
 38. Teske AJ, De Boeck BWL, Olimulder M et al. Echocardiographic assessment of regional right ventricular function: a head-to-head comparison between 2-dimensional and tissue Doppler-derived strain analysis. *J Am Soc Echocardiogr*, 2008; 21: 275–283. doi: [10.1016/j.echo.2007.08.027](https://doi.org/10.1016/j.echo.2007.08.027).
 39. Fine NM, Chen L, Bastiansen PM et al. Reference values for right ventricular strain in patients without cardiopulmonary disease: a prospective evaluation and meta-analysis. *Echocardiography*, 2015; 32: 787–796. doi: [10.1111/echo.12806](https://doi.org/10.1111/echo.12806).
 40. Bansal M, Cho G-Y, Chan J et al. Feasibility and accuracy of different techniques of two-dimensional speckle based strain and validation with harmonic phase magnetic resonance imaging. *J Am Soc Echocardiogr*, 2008; 21: 1318–1325. doi: [10.1016/j.echo.2008.09.021](https://doi.org/10.1016/j.echo.2008.09.021).
 41. Cameli M, Righini FM, Lisi M et al. Comparison of right versus left ventricular strain analysis as a predictor of outcome in patients with systolic heart failure referred for heart transplantation. *Am J Cardiol*, 2013; 112: 1778–1784. doi: [10.1016/j.amjcard.2013.07.046](https://doi.org/10.1016/j.amjcard.2013.07.046).
 42. Blanc J, Stos B, de Montalembert M et al. Right ventricular systolic strain is altered in children with sickle cell disease. *J Am Soc Echocardiogr*, 2012; 25: 511–517. doi: [10.1016/j.echo.2012.01.011](https://doi.org/10.1016/j.echo.2012.01.011).
 43. Muraru D, Onciul S, Peluso D et al. Gender- and method-specific reference values for right ventricular strain by two-dimensional speckle-tracking echocardiography. *Circ Cardiovasc Imaging*, 2016; 9: e003866. doi: [10.1161/CIRCIMAGING.115.003866](https://doi.org/10.1161/CIRCIMAGING.115.003866).
 44. Hayabuchi Y, Sakata M, Kagami S. Right ventricular myocardial deformation patterns in children with congenital heart disease associated with right ventricular pressure overload. *Eur Heart J Cardiovasc Imaging*, 2015; 16: 890–899. doi: [10.1093/ehjci/jev011](https://doi.org/10.1093/ehjci/jev011).
 45. Atsumi A, Ishizu T, Kameda Y et al. Application of 3-dimensional speckle tracking imaging to the assessment of right ventricular regional deformation. *Circ J*, 2013; 77: 1760–1768.
 46. Smith BCF, Dobson G, Dawson D et al. Three-dimensional speckle tracking of the right ventricle: toward optimal quantification of right ventricular dysfunction in pulmonary hypertension. *J Am Coll Cardiol*, 2014; 64: 41–51. doi: [10.1016/j.jacc.2014.01.084](https://doi.org/10.1016/j.jacc.2014.01.084).
 47. Rajagopalan N, Dohi K, Simon MA et al. Right ventricular dyssynchrony in heart failure: a tissue Doppler imaging study. *J Card Fail*, 2006; 12: 263–267. doi: [10.1016/j.cardfail.2006.02.008](https://doi.org/10.1016/j.cardfail.2006.02.008).
 48. Kalogeropoulos AP, Georgiopoulou VV, Howell S et al. Evaluation of right intraventricular dyssynchrony by two-dimensional strain echocardiography in patients with pulmonary arterial hypertension. *J Am Soc Echocardiogr*, 2008; 21: 1028–1034. doi: [10.1016/j.echo.2008.05.005](https://doi.org/10.1016/j.echo.2008.05.005).
 49. Badagliacca R, Reali M, Poscia R et al. Right intraventricular dyssynchrony in idiopathic, heritable, and anorexigen-induced pulmonary arterial hypertension: clinical impact and reversibility. *J Am Coll Cardiol Cardiovasc Imaging*, 2015; 8: 642–652. doi: [10.1016/j.jcmg.2015.02.009](https://doi.org/10.1016/j.jcmg.2015.02.009).
 50. Voelkel NF, Quaife RA, Leinwand LA et al. Right ventricular function and failure: report of a national heart, lung, and blood institute working group on cellular and molecular mechanisms of right heart failure. *Circ*, 2006; 114: 1883–1891. doi: [10.1161/CIRCULATIONAHA.106.632208](https://doi.org/10.1161/CIRCULATIONAHA.106.632208).
 51. Addetia K, Maffessanti F, Yamat M et al. Three-dimensional echocardiography-based analysis of right ventricular shape in pulmonary arterial hypertension. *Eur Heart J Cardiovasc Imaging*, 2016; 17: 564–575. doi: [10.1093/ehjci/jev171](https://doi.org/10.1093/ehjci/jev171).

Cite this article as: Surkova E, Peluso D, Kasprzak JD, Badano LP. Use of novel echocardiographic techniques to assess right ventricular geometry and function. *Kardiol Pol*, 2016; 74: 507–522. doi: [10.5603/KP.a2016.0041](https://doi.org/10.5603/KP.a2016.0041).